Published in final edited form as:
J Neurosci. 2011 October 26; 31(43): 15397–15406. doi:10.1523/JNEUROSCI.2196-11.2011.

Enhanced oscillatory activity in the hippocampal-prefrontal network is related to short-term memory function after early-life seizures

Jonathan K. Kleen[1], **Edie X. Wu**[1], **Gregory L. Holmes**[1,*], **Rod C. Scott**[1,2], and **Pierre-Pascal Lenck-Santini**[1]

[1]Department of Neurology, Neuroscience Center at Dartmouth, 518 East Borwell Building, Dartmouth Medical School, Hanover, New Hampshire 03755

[2]UCL, Institute of Child Health, 30 Guilford Street, WC1N 1EH, London, United Kingdom

Abstract

Neurological insults during development are associated with later impairments in learning and memory. Although remedial training can help restore cognitive function, the neural mechanisms of this recovery in memory systems are largely unknown. To examine this issue we measured electrophysiological oscillatory activity in the hippocampus (both CA3 and CA1) and prefrontal cortex of adult rats that had experienced repeated seizures in the first weeks of life, while they were remedially trained on a delayed-nonmatch-to-sample memory task. Seizure-exposed rats showed initial difficulties learning the task but performed similar to control rats after extra training. Whole-session analyses illustrated enhanced theta power in all three structures while seizure rats learned response tasks prior to the memory task. Whilst performing the memory task, dynamic oscillation patterns revealed that prefrontal cortex theta power was increased among seizure-exposed rats. This enhancement appeared after the first memory training steps using short delays and plateaued at the most difficult steps which included both short and long delays. Further, seizure rats showed enhanced CA1-prefrontal theta coherence in correct trials compared to incorrect trials when long delays were imposed, suggesting increased hippocampal-prefrontal synchrony for the task in this group when memory demand was high. Seizure-exposed rats also showed heightened gamma power and coherence among all three structures during the trials. Our results demonstrate the first evidence of hippocampal-prefrontal enhancements following seizures in early development. Dynamic compensatory changes in this network and interconnected circuits may underpin cognitive rehabilitation following other neurological insults to higher cognitive systems.

Introduction

The remarkable ability of the nervous system to adapt to insults or deprivation is believed to originate from plasticity phenomena. Extensive training can restore functional deficits in the neocortex following sensory disruption in early development through compensatory neuroplasticity (Zhou and Merzenich, 2009; Merabet and Pascual-Leone, 2010). However, the mechanisms underlying restoration of higher cognitive functions such as learning and memory after neuronal insults (Markowitsch et al., 1985; Gathercole and Alloway, 2006) are still poorly understood, particularly within cortical-limbic networks.

[*]Correspondence to: Gregory L. Holmes, M.D., Dartmouth Medical School, 518 East Borwell Building, 1 Medical Center Drive, Lebanon, New Hampshire 03756, Telephone: 603-650-4211, Fax: 603-650-6233, Gregory.L.Holmes@Dartmouth.edu.

Conflict of interest: None.

Patients that experienced neurological insults during development often develop compensatory cognitive strategies that help circumvent functional deficits (Mateer et al., 1996; Stiles et al., 1997). Subsequent cognitive improvements following a neurological insult are likely related to functional reorganization of neural circuits and adjustments in their dynamic coordination (Bach-y-Rita, 1990; Carmichael et al., 2001; Keller and Just, 2009). This plasticity can be measured on a network level *in vivo* through the quantification of oscillatory activity in local field potentials (Tsanov and Manahan-Vaughan, 2009; Voytek et al., 2010). Oscillations provide indices of ongoing neural processing among groups of neurons near the recording site (Mormann et al., 2005; Wang, 2010). In particular, hippocampal theta (4–12 Hz) and gamma (30–120 Hz) oscillations in the hippocampus and prefrontal cortex (PFC) have been correlated with short-term memory processing in rats (Jones and Wilson, 2005; Montgomery and Buzsaki, 2007; Adhikari et al., 2010) with analogous findings in humans (Canolty et al., 2006; Rizzuto et al., 2006; Watrous et al., 2011). In turn, pathological disruption of the hippocampus produces altered oscillatory activity which can parallel reduced cognitive ability (Chauviere et al., 2009; Marcelin et al., 2009; Adhikari et al., 2010; Sigurdsson et al., 2010; Voytek et al., 2010).

Given the critical role of the hippocampal-PFC network in short-term memory function, we examined whether memory training following a neurological insult during development produces neuroplastic changes in this system. We show that adult rats exposed to early-life seizures (ELS) indeed demonstrate altered evolution of oscillation characteristics in the hippocampus and PFC during training for a memory task. Moreover, following remedial training these rats show enhanced levels of select theta and gamma theta oscillations during trials compared to controls, as well as a relationship between CA1-PFC coherence and accuracy. These differences may reflect an inter-structure compensatory mechanism following neurological insults via hippocampal-PFC plasticity.

Methods

Animals and seizure model

Ten Sprague-Dawley rats of either sex were born in-house with half (N=5) experiencing 100 flurothyl-induced seizures during postnatal days 15–30 (6–7 seizures per day). This procedure is a model of ELS in humans (Isaeva et al., 2006), with normal subsequent phenotypic development to adulthood and no spontaneous seizures or epileptiform abnormalities on electroencephalogram (EEG) recordings. Control rats (N=5) did not receive seizures but were separated from the dam rat for the same amount of time. In adulthood (between postnatal days 100–120) all rats were implanted with electrodes in the CA3, CA1, and PFC on the right side. Following 1 week of surgical recovery, rats were food-restricted to 85% of their free-feeding weights, after which behavioral training commenced with EEG recorded from the three structures continuously during all sessions (Figure 1*A*, *B*). All animal procedures were approved by the Dartmouth Institutional Animal Care and Use Committee in accordance with National Institutes of Health guidelines, among conditions approved by the U.S. Department of Agriculture and the Association for Assessment and Accreditation of Laboratory Animal Care.

Surgery

Rats were anesthetized with isoflurane (2–3% in oxygen) and custom tetrodes with 0.5mm vertical span (to encompass the CA strata) were implanted in the dorsal-intermediate hippocampal CA3 (Figure 1*C*; deepest tip at 4.5mm lateral, 4.2mm posterior, and 5.0mm ventral from the bregma skull fissure; Paxinos and Watson, 2005) and CA1 (Figure 1*D*; deepest tip at 3.0mm lateral, 4.2mm posterior, and 2.9mm ventral). In addition, similar tetrodes with 1.5mm vertical span (to encompass the prelimbic area) were implanted in the

PFC (Figure 1*E*; deepest tip at 0.6mm lateral, 3.2mm anterior, and 4.6mm ventral). Ground wires were soldered to bone screws, and reference wires were implanted in the cerebellum for each rat. All wires were plugged into an interconnect socket array (Mill-Max Mfg. Corp., Oyster Bay, NY), and encased in dental cement.

Electrophysiology

Electrodes consisted of four 25μm nichrome wires (California Fine Wire, Grover Beach, CA), held in a 25-gauge stainless steel guide tube (Small Parts Inc., Miami Lakes, FL). Operational amplifiers plugged directly to the rat connector (unity gain), and EEG signals were transmitted via a custom cable and a rotating commutator (Dragonfly Research & Development Inc., Ridgeley, WV), all referenced to the cerebellum electrode. Recordings were made in an operant chamber described previously (Kleen et al., 2010). During all sessions, EEG signals were recorded from 2 leads in each structure and amplified at 1000x gain before digitization at 2315 Hz (DigiData 1322, Axon Instruments, Foster City, CA). Two electrodes were recorded in each structure so that power and coherence analyses could be performed on the EEG signal from the most appropriately placed electrode, verified by histology before analysis.

Behavior

Rats sought food rewards in all tasks (45 mg Noyes food pellet; Research Diets, Incorporated, New Brunswick, NJ). Training sessions were run at approximately the same time each day for each rat. Behavioral tasks that made up the training step sequence are listed in order on the x-axis in Figure 2*A* and have been described previously (Brown and Jenkins, 1968; Kleen et al., 2010). The first step in response training was the “autoshape” step, which encouraged lever pressing by pairing the lever with a food reward (Brown and Jenkins, 1968). Specifically, the lever was extended into the chamber and then retracted either after the rat pressed the lever or 5 seconds had elapsed, followed by a food reward in both cases. This training step was followed by two fixed-ratio schedules, in which the rat was required to press the lever or break an infrared beam in the nosepoke apparatus to gain a food reward. The fourth step involved a sequence of lever-nosepoke-opposite lever to gain a food reward, preparing the rat for the action sequence of the upcoming delayed-nonmatch-to-sample (DNMS) task trials. Rats were required to gain a certain number of food rewards in a specified amount of time to advance to the next step, and these criteria were the same for all rats. Specifically, >25 responses within 45 min were needed in both the autoshape and lever press steps, >10 beam-breaks in 30 min for the nosepoke step, and >40 completed sequences in 45 min for the lever-nosepoke-opposite lever step.

All subsequent DNMS sessions were made up of 50 trials, and lasted 45 min each, in which the rats were required to perform at least 40 trials correctly (80%) to advance to the next training step. A DNMS trial (Figure 1*F*) consisted of one lever (right or left) being randomly presented to the rat at first. Upon pressing the sample lever, the rat then had to break an infrared beam (nosepoke) on the opposite wall of the chamber. Immediately after the beam was broken, both levers were presented. A correct response was defined as pressing the lever that was not presented earlier as the sample (i.e. non-match-to-sample), which produced a food reward.

DNMS training sessions (DNMS Train in Figure 2*A*) began with a trial of DNMS, and if the animal performed it correctly, another was given, and so on. However, if the animal performed a trial incorrectly, the next trial was a lever-nosepoke-opposite lever trial (as in response training), followed immediately by another attempt at a DNMS trial. Following criterion performance (>80% successful trials), rats began DNMS-only sessions with no imposed delay at first (“Block 0”) and then progressively-increasing delay ranges. Delays

were imposed by designating nosepokes as unproductive until a specified amount of time had elapsed after the sample press. This specified delay period was randomly selected in each trial, from a range that was defined for each DNMS block. The delay ranges for each block were as follows: Block 1, 1–5 sec; Block 2, 1–10 sec; Block 3, 1–15 sec; Block 4, 1–20 sec; Block 5, 1–25 sec; Block 6, 1–30 sec.

Data analysis

A repeated-measures ANOVA assuming a Poisson distribution for counts was used to evaluate the number of sessions taken to successfully complete the training steps. Accuracy and reaction time were analyzed using logistic regression adjusted for within-animal correlations, with each DNMS trial treated as an individual observation (N=5041 trials). Developmental and dynamic oscillation measures were analyzed using repeated-measures ANOVAs, with treatment and time as main effects, and an interaction term. Two ELS rats were not incorporated into oscillation analyses due to unreliable headstage connections. Sessions with substantial electrical noise (e.g. ground artifact) or in which rats showed clear preferences for one lever (i.e. non-memory strategies) were not utilized in dynamic oscillation analyses.

Oscillation development: Power and coherence spectrograms were calculated with the entire EEG data traces from each behavioral session, using multi-taper Fourier transform estimates on non-overlapping windows (1 sec for theta, 0.1 sec for gamma). Custom software was written for these analyses using Matlab (The Mathworks, Inc., Natick, MA), built upon base software provided by Chronux (Mitra and Bokil, 2008; http://www.chronux.org). Power spectrograms (time × frequency × power) were generated for power results within each brain area (CA3, CA1, and PFC), and coherence spectrograms (time × frequency × coherence) were generated separately for CA3-CA1 signals and CA1-PFC signals. Frequency indices calculated from the initial window size were then used to extract the data within the theta and gamma bands separately. Resulting data within the active behavioral session (time-locked to behavioral event signals from the chamber interface) were summed (power) or averaged (coherence) across frequencies bands of 4–12 Hz for theta and 30–50 Hz for gamma. This produced a linear time vector for each measure over the length of the session with data points at 1-second intervals for theta and 0.1 second intervals for gamma. The medians of these vectors were taken as the general power and coherence values for that session. These values were then normalized by the values from the first session (the “autoshape” session; see Behavior section in Methods and group averages in Figure 4*A*, *C*) to allow visualization of changes from baseline over time.

Dynamic oscillation analysis

Continuous wavelet transforms were calculated on segments of EEG data (down-sampled by a factor of four to a 579 Hz sampling rate) that began 6 sec before the sample press and end 6 sec after the match press for each trial. Custom software was written for these analyses using Matlab, built upon base software provided by Aslak Grinsted (Arctic Centre, University of Lapland, Finland; Grinsted et al., 2004). Wavelet estimation allowed similar representation of power and coherence as time-frequency spectrograms, yet with time resolution equal to that of the raw data traces. The Morlet wavelet was used to provide a balance between time and frequency resolution. This wavelet function has been used in previous studies of theta and gamma oscillations (Colgin et al., 2009; Montgomery and Buzsaki, 2007). Specific features of the wavelet analysis employed here are described in Grinsted et al. (2004). For each trial, wavelet power spectrograms were generated for the CA3, CA1, and PFC regions; coherence spectrograms were also generated for CA3-CA1 and CA1-PFC signals. Frequency indices calculated from period scaling factors were then used to extract the data within the theta and gamma bands. This data was summed (power)

or averaged (coherence) across the data within the theta band frequencies and across the data within the gamma band frequencies (30–50 Hz). The resultant vectors were dynamic (real-time) time-series of summed power or average coherence data, which was then smoothed using a 0.5 sec (theta) or 0.2 sec (gamma) moving average. To avoid edge estimations defined by the cone of influence in wavelet analyses (Grinsted et al., 2004), the first and last second of each data segment were removed. The resulting dynamic oscillation estimate for each trial was then down-sampled to 10 Hz for statistical analyses, and normalized by the corresponding pre-trial baseline. Only trials with delays between 10–30 seconds were used to ensure appropriate time allocation for encoding, maintenance and retrieval processes (Kleen et al., 2010). Each rat's data was averaged across trials with delays between 10–30 sec (N=3313 trials) to adjust to equal weights for analysis. Data periods between −1.5 sec to 5 sec around the sample press, and −5 sec to 0 sec before the match press were analyzed to encompass memory encoding, maintenance, and retrieval.

Results

Learning impairments and subsequent recovery in ELS rats

Rats were trained on each step until criterion performance had been attained in a session (i.e. remedial training; see Methods), whereupon they advanced to the next training step. Learning abilities were thereby indexed by the number of sessions taken to advance through the consecutive training steps over time. The groups performed similarly during response training but ELS rats required significantly more DNMS Train sessions to achieve criterion performance ($p<0.01$, Figure 2*A*), in agreement with previous studies on ELS and hippocampal-dependent task deficits (Holmes, 2009; Karnam et al., 2009a; Karnam et al., 2009b). Following eventual acquisition of the DNMS task (80% correct in DNMS Training; see Methods) via remedial training, ELS rats paralleled controls in learning the more difficult DNMS steps (Blocks 0–4 in Figure 2*A*). Data for Blocks 5 and 6 are not shown in Figure 2*A* since some animals experienced electrode headstage malfunctions before passing criterion for those later blocks, skewing the group averages and standard errors upon illustration. All animals increased in accuracy as training progressed over the consecutive DNMS blocks, with no difference in overall accuracy between the groups ($p=0.58$; Figure 2*B*) using logistic regression on 5041 trials adjusted for within-animal correlations. As in previous studies (Hampson et al., 1999; Kleen et al., 2010), delay was the main predictor of accuracy ($p<0.001$, odds ratio [OR], 1.06; 95% CI, 1.04–1.07; Figure 2*C*), with longer delays decreasing the likelihood of correct responses. Neither reaction time (the amount of time taken to press the match lever after it was extended into the chamber) nor the distribution of delays differed between ELS and control rats ($p=0.14$ and $p=0.17$ respectively). Further, the relation between session step and time to complete a session did not differ between the groups ($p=0.15$), indicating similar speeds and activity levels.

Altered evolution of power and coherence in ELS rats during task acquisition

We measured oscillation bands of 4–12 Hz for theta and 30–50 Hz for gamma in this study because this latter range ("low gamma") is specifically involved in CA3-CA1 coordination (Colgin et al., 2009). Analysis of raw power (Figure 3*A–C, F*) and coherence (Figure 3*D, E, G*) revealed characteristic theta and gamma oscillation peaks in the CA3, CA1 and PFC (Colgin et al., 2009; Sigurdsson et al., 2010). Raw median power and coherence measures for oscillation power and coherence were calculated for each session using Fourier-based analyses and averaged across frequencies within the theta and gamma bands. These did not differ statistically between the groups in any of the structures during the first behavioral session except for CA3 gamma power 1($p<0.05$). However, raw power and coherence can be influenced by small variations in electrode placement, and since the goal of our study was to assess changes in oscillation measures over the course of training (see Methods), we

normalized all subsequent session values by the first training step to adjust for these potential differences.

By the end of response training, ELS animals showed robust increases in both theta power in the CA3, CA1, and PFC compared to controls ($p<0.001$ for all; see Figure 4*A*). CA1 gamma power also increased in this group during this period while controls remained at baseline (Figure 4*B*). Thus, ELS rats displayed atypically enhanced local oscillation power during response training (Pych et al., 2005).

As training progressed into the consecutive DNMS steps, control rats showed increased PFC theta power and decreased CA3 theta power ($p<0.001$; Figure 4*A*). Meanwhile ELS animals maintained increases in both CA3 and CA1 theta power ($p<0.001$). Furthermore, while both groups showed increased gamma power in the CA1 and PFC (Figure 4*B*), ELS rats also showed significantly increased CA3 gamma power ($p<0.001$). A clear increase in CA3-CA1 gamma coherence across the DNMS steps in control rats diverged from ELS rats which remained at baseline levels ($p<0.001$). Meanwhile, ELS rats also developed a steady increase in CA1-PFC theta coherence that was not significant in controls ($p<0.001$; Figure 4*A*). In other words, while changes in the intrahippocampal systems were observed in controls during DNMS training, ELS rats showed more general enhancement of the hippocampal-PFC network.

Alternate dynamic oscillation patterns among ELS rats during DNMS trials

Differences in general oscillation development during training suggest that alternate cognitive strategies may be emerging. To establish whether dynamic oscillation patterns during trials differed between the groups, we next examined dynamic power and coherence differences between the groups during trial performance using wavelet analysis. This provided a continuous temporal resolution (N=3313 trials adjusted for individual rats; Figure 5). These measures were time-locked to the sample and match presses, and normalized for each trial by dividing by a pre-trial baseline (−5 to −2.5 sec before the sample press) to adjust for initial differences between rats and across sessions as evidenced in Figure 4. Pre-trial baseline values for power and coherence did not show consistent changes over the course of training for any of the power or coherence measures.

The dynamic patterns of control animals in Figure 6*A* (blue curves) illustrate the general functional modulation of theta oscillations in the DNMS task. Specifically, decreases in theta power and coherence among all structures were evident at the time of the sample press, followed by increased theta power in all structures immediately afterward as the rat turned to the other side of the chamber for the delay period ($p<0.001$ for all; repeated measures ANOVA adjusted within-animal; Figure 6*A*). In the seconds preceding the match press, CA1-PFC theta coherence was persistently increased from pre-trial baselines ($p<0.001$) but returned to baseline at the end of the trial, confirming previous studies of short-term memory tasks in rats (Jones and Wilson, 2005; Sigurdsson et al., 2010). Decreases in gamma power and coherence were seen among nearly all structures before and after the sample press, and shortly before the match press ($p<0.001$ for all; Figure 7*A*).

We then examined divergences of ELS rat oscillation patterns (red curves in Figure 6*A*) from controls. All ELS rats showed increases in PFC cortex power that began at the trial initiation culminated to highest levels shortly before the match press ($p<0.001$) and converged with controls after the trial. CA1-PFC theta coherence was also markedly increased compared to controls around the sample press ($p<0.001$). Moreover, gamma power and coherence were increased among all structures in ELS animals compared to their control counterparts during the trials ($p<0.001$ for all; Figure 7*A*), returning to control levels immediately after trials were complete. These oscillatory activity enhancements among ELS

rats during trials reveal heightened involvement and coordination of the hippocampal-PFC network during short-term memory processing.

We then examined at which point these differences may have arisen during the course of training. Many of the biggest differences in dynamic oscillations between control and ELS animals occurred during the −4 and −2 s preceding the match press (grey box in Figure 6*A*), i.e. around the time the animal had to recall which lever it had pressed previously. Thus for each power and coherence measure, we averaged this period to a single value in each trial (again normalized to the pre-trial baseline), and then quantified how these levels changed over the course of training by grouping the DNMS training blocks into three consecutive levels - Blocks 0–1, 2–3, and 4–6. Figure 6*B* reveals that PFC theta power is similar between the groups in Blocks 0–1 and that it increases in ELS rats in Blocks 2 and 3, reaching its highest levels during Blocks 4, 5 and 6. A repeated measures ANOVA showed an increasing trend among all rats ($p=0.056$), and confirmed a treatment effect in this measure ($p<0.001$). No other theta power or coherence measures were statistically significant ($p>0.05$ for all), in agreement with the dynamic envelopes in Figure 6*A*.

We analyzed gamma evolution over time using the same time period during the trial (grey box in Figure 7*A*). CA3 power (repeated measures ANOVA; $p<0.05$), CA3-CA1 coherence ($p<0.01$), CA1 power ($p<0.001$), CA1-PFC coherence ($p<0.01$), and PFC power ($p<0.05$) were consistently elevated levels among ELS rats across all blocks (Figure 7*B*). CA3-CA1 gamma coherence additionally showed a trend toward increasing levels over the training blocks ($p=0.057$) when an interaction term for treatment versus block was factored into the statistical model.

We next examined the influence of trial difficulty on the EEG oscillation measures by analyzing the same data (corresponding to the grey boxes in Figures 6*A* and 7*A*) grouped in delays of increasing duration: 10–15 sec, 15–20 sec, 20–25 sec, and 25–30 sec. Across all levels of delay, ELS animals showed significantly higher values of PFC theta power ($p<0.001$) and all gamma power and coherence measures ($p<0.01$ for all) compared to controls. However, no theta or gamma oscillation measures were significantly modulated by delay nor were any interactions present between delay and treatment group.

CA1-PFC coherence predicted memory performance in ELS but not control rats

To confirm the functional relevance of these oscillation patterns, we compared correct versus incorrect trials. In trials with longer delays (20–30 sec), CA1-PFC coherence was markedly increased among correct trials relative to incorrect trials in ELS rats but not in controls (Figure 8*A, B*). This trend was absent in both groups among short delays (10–20 sec; Figure 8*C*), and other measures of theta and gamma power and coherence did not show this degree of performance modulation. These results indicate that ELS rats had increased hippocampal-PFC interplay when memory demand was high (Lee and Kesner, 2003).

Discussion

We showed that following a neurological insult early in life, the recovery of cognitive performance in adult rats is associated with the development of distinct patterns of brain oscillations in the hippocampal-PFC network. ELS rats showed altered theta and gamma oscillations compared to controls, in both general development during task acquisition and dynamic activity patterns during task performance. Some of the dynamic measures were unequivocally observed in all ELS rats (Figure 6*C*) suggesting a stereotyped neural adaptation to the insult.

ELS rats exhibited initial impairments relative to controls in learning the DNMS task as expected following this neurological insult (Holmes, 2009; Karnam et al., 2009a; Karnam et al., 2009b), but were able to perform as well as controls with increasing delays on the remedial training paradigm (Blocks 0–6). We first measured baseline power and coherence among all structures in the first session, noting similar values in all but CA3 power which was lower among ELS animals. Although the recording sites were verified through post-mortem histology, it is not clear whether a different baseline between the groups could be caused by ELS or simply due to variations in electrode placement within the structures of interest. However the goal of this study was to assess changes in EEG oscillation patterns over the course of training and during real-time performance of DNMS trials, thus we used normalized power and coherence measures to allow visualization of these fluctuations.

We noted divergences of general levels of theta power in all structures during response learning and of CA3-CA1 gamma coherence during DNMS acquisition (Figures 4*B* and *D* respectively). These findings demonstrate that experience-dependent changes in oscillation coordination were emerging in ELS animals over the course of training. However, general averages in the whole-session analysis (Figure 4) do not directly assess the functional activity pattern modifications that are critical for task performance. To examine whether the EEG activity patterns during real-time performance differed between the groups, we performed the dynamic analyses depicted in Figures 5–8.

We uncovered a number of group differences that suggested that the maintenance of performance in ELS animals may have arisen via compensatory processing in auxiliary networks. In particular, ELS rats demonstrated large increases in PFC theta power which developed in the more difficult DNMS training stages (Blocks 2–6). Additionally, all structures showed variable increases in gamma power and coherence that persisted during the task, implying stronger local information processing in these areas (Beshel et al., 2007; Colgin and Moser, 2010). Furthermore, enhanced CA1-PFC coherence was related to enhanced performance in the more difficult trials (longer delays). This effect was not seen in control rats, suggesting that ELS animals in particular may have relied upon increased hippocampal-PFC communication when the task demand was high.

Although we could not measure running speed due to confinements in the operant chamber, potential disparities in movement between groups likely impart little to no influence on our results in part given equivalent measures of activity such as reaction time and time to complete sessions. Moreover, we noted similar group levels of dynamic CA1 theta power (Figure 6*A*, *B*), which is known to be modulated by speed and movement (McFarland et al., 1975) in addition to learning and memory processing (Montgomery et al., 2009). Our interpretation and conclusions here relate mainly to findings regarding PFC theta power and CA1-PFC coherence, and we are not aware of literature clearly linking these measurements to movement or running speed similar to CA1 theta power.

Abnormal alterations in local networks can induce neuroplasticity to recruit auxiliary networks or enhance existing functional networks for effective computation (Feldman, 2009). Previous work shows that rats exposed to ELS have consistent alterations in hippocampal cellular and synaptic properties later in life that relate to cognitive dysfunction (de Rogalski Landrot et al., 2001; Cornejo et al., 2007). The ELS rats in this study showed disparate PFC-related theta oscillation patterns, suggesting that they may have adapted to faulty hippocampal circuitry by developing a more frontal lobe-reliant strategy (Lee and Kesner, 2003). When task demands required retrieval of memory after a longer delay, hippocampal interplay (i.e. CA1-PFC coherence) may have served to reconcile discrepant information (Wall and Messier, 2001). This compensatory possibility has been hypothesized in lesion studies of the hippocampus and PFC (Lee and Kesner, 2003; Wang and Cai, 2006),

and we provide evidence here via dynamic electrophysiological activity profiles within this network during task performance.

The network mechanisms for the performance of delayed-match and nonmatch paradigms have been examined in both animal and human settings. Lesion studies have emphasized the clear role of the hippocampal circuitry in these paradigms (Kirby & Higgins, 1998; Hampson et al., 1999), as well as PFC contributions (Joel et al., 1997). Work using single-unit activity (Hampson et al. 1993; Hampson & Deadwyler, 1996) showed that neurons in the hippocampus respond selectively to events in the DNMS, such as specific phases of the task (sample vs. press) or behavioral events (nose-poke or bar press). It has been shown that medial PFC neurons can be entrained to hippocampal theta frequency (Siapas et al., 2005; Hyman et al., 2005), and there is now strong evidence that this entrainment is involved in learning and memory in various working memory tasks (Jones and Wilson, 2005; Hyman et al., 2010; Benchenane et al, 2010). Kojima and Goldman-Rakic (1982) noted that PFC neurons exhibiting spatial-related firing properties tend to fire most strongly in the first few seconds of the delay period for a spatial delayed-response task. Perhaps in line with this, control rats in our study showed increased PFC theta at about one second into the delay but then dropped back to pre-trial baseline levels. ELS rats showed increased PFC theta (and CA1-PFC theta in correct trials with long delays) immediately after the sample press and their levels did not return to baseline until one second before the match press. This implies that although the PFC may be important for short- or no-delay versions of DNMS under normal conditions, ELS rats engage this structure more persistently throughout trials. Together, these results demonstrate that increases in hippocampus and PFC coordination and PFC activity may support performance in the DNMS task after a neurological insult early in life.

Large increases of PFC theta power in ELS rats during the delay likely reflect more of an adjunct to hippocampal-mediated memory function, not a replacement. The PFC maintains several cognitive facets including attention, working memory, vigilant sensory encoding, rehearsal processing, and behavioral flexibility (Awh and Jonides, 2001; Floresco et al., 2009). In fact, during the delay period of a short-term memory task, the proportion of PFC neuronal activity related to attention is higher than that of memory function (Lebedev et al., 2004). Here, PFC theta power in ELS rats was persistently elevated during the entire length of the trial suggesting it may reflect increased attention during active performance. This pattern is similar to activation profiles of the dorsolateral PFC in humans during the delay of a working memory task, attributed to both memory and attention processes in this region (Curtis and D'Esposito, 2003). Thus, the functional significance of enhanced PFC neural activity observed in this study likely involves an array of interplaying cognitive faculties during the execution of the DNMS task including attention and working memory (Matzel and Kolata, 2010).

Regardless of putative cognitive strategies, distinct oscillation patterns between ELS and control rats during trials demonstrates different neural coordination to solve the task following a neurological insult. These disparities could reflect a compensation between multiple limbic (e.g. hippocampus) and neocortical (e.g. PFC) structures via neural plasticity (Bach-y-Rita, 1990), revealed here by oscillatory network activity (Voytek et al., 2010) in the hippocampal-PFC network. This is particularly supported by the observation that these patterns developed in response to DNMS training and by the relation between accuracy and heightened CA1-PFC theta activity in ELS animals but not among controls.

Overall, our findings demonstrate that following a neurological insult early in life learning and performance may become mediated through alternate yet equally effective neural oscillation pathways, even in fully mature animals. Compensatory neural strategies could be

capitalized upon to accelerate cognitive rehabilitation in neurological disorders (Mateer et al., 1996; Stiles et al., 1997). For example, our data suggests that individuals who experienced ELS and have chronic memory impairments may benefit from cognitive training on PFC-mediated functions (e.g. working memory and attentional elements) to aid short-term memory. ELS affect 4% of the population, and nearly 70% of these individuals go on to develop cognitive impairment later in life (Legido et al., 1991; Hauser, 1995) indicating that a substantial number of individuals could benefit from these types of tailored interventions. Our study encourages the investigation of alternate neural strategies in other models of neurological disease, using oscillatory activity as an effective surrogate for network activity (Adhikari et al., 2010; Sigurdsson et al., 2010; Voytek et al., 2010). This avenue will shed light on other brain networks that could compensate for stereotyped impairments, and could provide the neurophysiological basis for directed cognitive rehabilitation programs to accelerate and augment cognitive recovery.

Acknowledgments

We thank Peter Cuadrilla, Marcella Lucas, Forrest Miller, and Qian Zhao for assistance and support. This work was supported by the National Institutes of Health grants F30NS064624 (J.K.K.), R21MH086833 (P.P.L.S.), the Emmory R. Shapses Research Fund, R01NS044295, R01NS073083 (G.L.H.), and the Great Ormond Street Children's Charity (R.C.S.).

Abbreviations

DNMS	delayed-nonmatch-to-sample
EEG	electroencephalogram
ELS	early-life seizures
PFC	prefrontal cortex

References

Adhikari A, Topiwala MA, Gordon JA. Synchronized activity between the ventral hippocampus and the medial prefrontal cortex during anxiety. Neuron. 2010; 65:257–269. [PubMed: 20152131]

Awh E, Jonides J. Overlapping mechanisms of attention and spatial working memory. Trends Cogn Sci. 2001; 5:119–126. [PubMed: 11239812]

Bach-y-Rita P. Brain plasticity as a basis for recovery of function in humans. Neuropsychologia. 1990; 28:547–554. [PubMed: 2395525]

Benchenane K, Peyrache A, Khamassi M, Tierney PL, Gioanni Y, Battaglia FP, Wiener SI. Coherent theta oscillations and reorganization of spike timing in the hippocampal-prefrontal network upon learning. Neuron. 2010; 66(6):921–36. [PubMed: 20620877]

Beshel J, Kopell N, Kay LM. Olfactory bulb gamma oscillations are enhanced with task demands. J Neurosci. 2007; 27:8358–8365. [PubMed: 17670982]

Brown PL, Jenkins HM. Auto-shaping of the pigeon's key-peck. J Exp Anal Behav. 1968; 11:1–8. [PubMed: 5636851]

Canolty RT, Edwards E, Dalal SS, Soltani M, Nagarajan SS, Kirsch HE, Berger MS, Barbaro NM, Knight RT. High gamma power is phase-locked to theta oscillations in human neocortex. Science. 2006; 313:1626–1628. [PubMed: 16973878]

Carmichael ST, Wei L, Rovainen CM, Woolsey TA. New patterns of intracortical projections after focal cortical stroke. Neurobiol Dis. 2001; 8:910–922. [PubMed: 11592858]

Chauviere L, Rafrafi N, Thinus-Blanc C, Bartolomei F, Esclapez M, Bernard C. Early deficits in spatial memory and theta rhythm in experimental temporal lobe epilepsy. J Neurosci. 2009; 29:5402–5410. [PubMed: 19403808]

Colgin LL, Moser EI. Gamma oscillations in the hippocampus. Physiology (Bethesda). 2010; 25:319–329. [PubMed: 20940437]

Colgin LL, Denninger T, Fyhn M, Hafting T, Bonnevie T, Jensen O, Moser MB, Moser EI. Frequency of gamma oscillations routes flow of information in the hippocampus. Nature. 2009; 462:353–357. [PubMed: 19924214]

Cornejo BJ, Mesches MH, Coultrap S, Browning MD, Benke TA. A single episode of neonatal seizures permanently alters glutamatergic synapses. Ann Neurol. 2007; 61:411–426. [PubMed: 17323345]

Curtis CE, D'Esposito M. Persistent activity in the prefrontal cortex during working memory. Trends Cogn Sci. 2003; 7:415–423. [PubMed: 12963473]

de Rogalski Landrot I, Minokoshi M, Silveira DC, Cha BH, Holmes GL. Recurrent neonatal seizures: relationship of pathology to the electroencephalogram and cognition. Brain Res Dev Brain Res. 2001; 129:27–38.

DeCoteau WE, Thorn C, Gibson DJ, Courtemanche R, Mitra P, Kubota Y, Graybiel AM. Learning-related coordination of striatal and hippocampal theta rhythms during acquisition of a procedural maze task. Proc Natl Acad Sci U S A. 2007; 104:5644–5649. [PubMed: 17372196]

Feldman DE. Synaptic mechanisms for plasticity in neocortex. Annu Rev Neurosci. 2009; 32:33–55. [PubMed: 19400721]

Floresco SB, Zhang Y, Enomoto T. Neural circuits subserving behavioral flexibility and their relevance to schizophrenia. Behav Brain Res. 2009; 204:396–409. [PubMed: 19110006]

Gathercole SE, Alloway TP. Practitioner review: short-term and working memory impairments in neurodevelopmental disorders: diagnosis and remedial support. J Child Psychol Psychiatry. 2006; 47:4–15. [PubMed: 16405635]

Grinsted A, Moore JC, Jevrejeva S. Application of the cross wavelet transform and wavelet coherence to geophysical time series. Nonlin Processes Geophys. 2004; 11:561–566.

Hampson RE, Deadwyler SA. Ensemble codes involving hippocampal neurons are at risk during delayed performance tests. Proc Natl Acad Sci U S A. 1996; 93(24):13487–93. [PubMed: 8942961]

Hampson RE, Heyser CJ, Deadwyler SA. Hippocampal cell firing correlates of delayed-match-to-sample performance in the rat. Behav Neurosci. 1993; 107(5):715–39. [PubMed: 8280383]

Hampson RE, Jarrard LE, Deadwyler SA. Effects of ibotenate hippocampal and extrahippocampal destruction on delayed-match and -nonmatch-to-sample behavior in rats. J Neurosci. 1999; 19:1492–1507. [PubMed: 9952425]

Hauser WA. Epidemiology of epilepsy in children. Neurosurg Clin N Am. 1995; 6:419–429. [PubMed: 7670316]

Holmes GL. The long-term effects of neonatal seizures. Clin Perinatol. 2009; 36:901–914. vii–viii. [PubMed: 19944841]

Hyman JM, Zilli EA, Paley AM, Hasselmo ME. Working memory performance correlates with prefrontal-hippocampal theta interactions but not with prefrontal neuron firing rates. Front Integr Neurosci. 2010; 4:2. [PubMed: 20431726]

Isaeva E, Isaev D, Khazipov R, Holmes GL. Selective impairment of GABAergic synaptic transmission in the flurothyl model of neonatal seizures. Eur J Neurosci. 2006; 23:1559–1566. [PubMed: 16553619]

Joel D, Weiner I, Feld J. Electrolytic lesions of the medial prefrontal cortex in rats disrupt performance on an analog of the Wisconsin Card Sorting Test, but do not disrupt latent inhibition: implications for animal models of schizophrenia. Behav Brain Res. 1997; 85:187–201. [PubMed: 9105575]

Jones MW, Wilson MA. Theta Rhythms Coordinate Hippocampal–Prefrontal Interactions in a Spatial Memory Task. PLoS Biol. 2005; 3:e402. [PubMed: 16279838]

Karnam HB, Zhao Q, Shatskikh T, Holmes GL. Effect of age on cognitive sequelae following early life seizures in rats. Epilepsy Res. 2009a; 85:221–230. [PubMed: 19395239]

Karnam HB, Zhou JL, Huang LT, Zhao Q, Shatskikh T, Holmes GL. Early life seizures cause long-standing impairment of the hippocampal map. Exp Neurol. 2009b; 217:378–387. [PubMed: 19345685]

Keller TA, Just MA. Altering cortical connectivity: remediation-induced changes in the white matter of poor readers. Neuron. 2009; 64:624–631. [PubMed: 20005820]

Kirby DL, Higgins GA. Characterization of perforant path lesions in rodent models of memory and attention. Eur J Neurosci. 1998; 10:823–38. [PubMed: 9753151]

Kleen JK, Scott RC, Holmes GL, Lenck-Santini PP. Hippocampal interictal spikes disrupt cognition in rats. Ann Neurol. 2010; 67:250–257. [PubMed: 20225290]

Kojima S, Goldman-Rakic PS. Delay-related activity of prefrontal neurons in rhesus monkeys performing delayed response. Brain Res. 1982; 248(1):43–9. [PubMed: 7127141]

Lebedev MA, Messinger A, Kralik JD, Wise SP. Representation of attended versus remembered locations in prefrontal cortex. PLoS Biol. 2004; 2:e365. [PubMed: 15510225]

Lee I, Kesner RP. Time-dependent relationship between the dorsal hippocampus and the prefrontal cortex in spatial memory. J Neurosci. 2003; 23:1517–1523. [PubMed: 12598640]

Legido A, Clancy RR, Berman PH. Neurologic outcome after electroencephalographically proven neonatal seizures. Pediatrics. 1991; 88:583–596. [PubMed: 1881741]

Marcelin B, Chauviere L, Becker A, Migliore M, Esclapez M, Bernard C. h channel-dependent deficit of theta oscillation resonance and phase shift in temporal lobe epilepsy. Neurobiol Dis. 2009; 33:436–447. [PubMed: 19135151]

Markowitsch HJ, Kessler J, Streicher M. Consequences of serial cortical, hippocampal, and thalamic lesions and of different lengths of overtraining on the acquisition and retention of learning tasks. Behav Neurosci. 1985; 99:233–256. [PubMed: 3843710]

Mateer CA, Kerns KA, Eso L. Management of attention and memory disorders following traumatic brain injury. J Learn Disabil. 1996; 29:618–632. [PubMed: 8942306]

Matzel LD, Kolata S. Selective attention, working memory, and animal intelligence. Neurosci Biobehav Rev. 2010; 34:23–30. [PubMed: 19607858]

McFarland WL, Teitelbaum H, Hedges EK. Relationship between hippocampal theta activity and running speed in the rat. J Comp Physiol Psychol. 1975; 88:324–328. [PubMed: 1120805]

Merabet LB, Pascual-Leone A. Neural reorganization following sensory loss: the opportunity of change. Nat Rev Neurosci. 2010; 11:44–52. [PubMed: 19935836]

Mitra, P.; Bokil, H. Observed brain dynamics. Oxford; New York: Oxford University Press; 2008.

Montgomery SM, Betancur MI, Buzsaki G. Behavior-dependent coordination of multiple theta dipoles in the hippocampus. J Neurosci. 2009; 29:1381–94. [PubMed: 19193885]

Montgomery SM, Buzsaki G. Gamma oscillations dynamically couple hippocampal CA3 and CA1 regions during memory task performance. Proc Natl Acad Sci U S A. 2007; 104:14495–14500. [PubMed: 17726109]

Mormann F, Fell J, Axmacher N, Weber B, Lehnertz K, Elger CE, Fernandez G. Phase/amplitude reset and theta-gamma interaction in the human medial temporal lobe during a continuous word recognition memory task. Hippocampus. 2005; 15:890–900. [PubMed: 16114010]

Pych JC, Chang Q, Colon-Rivera C, Haag R, Gold PE. Acetylcholine release in the hippocampus and striatum during place and response training. Learn Mem. 2005; 12:564–572. [PubMed: 16322358]

Rizzuto DS, Madsen JR, Bromfield EB, Schulze-Bonhage A, Kahana MJ. Human neocortical oscillations exhibit theta phase differences between encoding and retrieval. Neuroimage. 2006; 31:1352–1358. [PubMed: 16542856]

Siapas AG, Lubenov EV, Wilson MA. Prefrontal phase locking to hippocampal theta oscillations. Neuron. 2005; 46(1):141–51. [PubMed: 15820700]

Sigurdsson T, Stark KL, Karayiorgou M, Gogos JA, Gordon JA. Impaired hippocampal-prefrontal synchrony in a genetic mouse model of schizophrenia. Nature. 2010; 464:763–767. [PubMed: 20360742]

Stiles J, Trauner D, Engel M, Nass R. The development of drawing in children with congenital focal brain injury: evidence for limited functional recovery. Neuropsychologia. 1997; 35:299–312. [PubMed: 9051678]

Tsanov M, Manahan-Vaughan D. Long-term plasticity is proportional to theta-activity. PLoS One. 2009; 4:e5850. [PubMed: 19513114]

Voytek B, Davis M, Yago E, Barcelo F, Vogel EK, Knight RT. Dynamic neuroplasticity after human prefrontal cortex damage. Neuron. 2010; 68:401–408. [PubMed: 21040843]

Wall PM, Messier C. The hippocampal formation--orbitomedial prefrontal cortex circuit in the attentional control of active memory. Behav Brain Res. 2001; 127:99–117. [PubMed: 11718887]

Wang GW, Cai JX. Disconnection of the hippocampal-prefrontal cortical circuits impairs spatial working memory performance in rats. Behav Brain Res. 2006; 175:329–336. [PubMed: 17045348]

Wang XJ. Neurophysiological and computational principles of cortical rhythms in cognition. Physiol Rev. 2010; 90:1195–1268. [PubMed: 20664082]

Watrous AJ, Fried I, Ekstrom AD. Behavioral Correlates of Human Hippocampal Delta and Theta Oscillations During Navigation. J Neurophysiol. 2011

Zhou X, Merzenich MM. Developmentally degraded cortical temporal processing restored by training. Nat Neurosci. 2009; 12:26–28. [PubMed: 19079250]

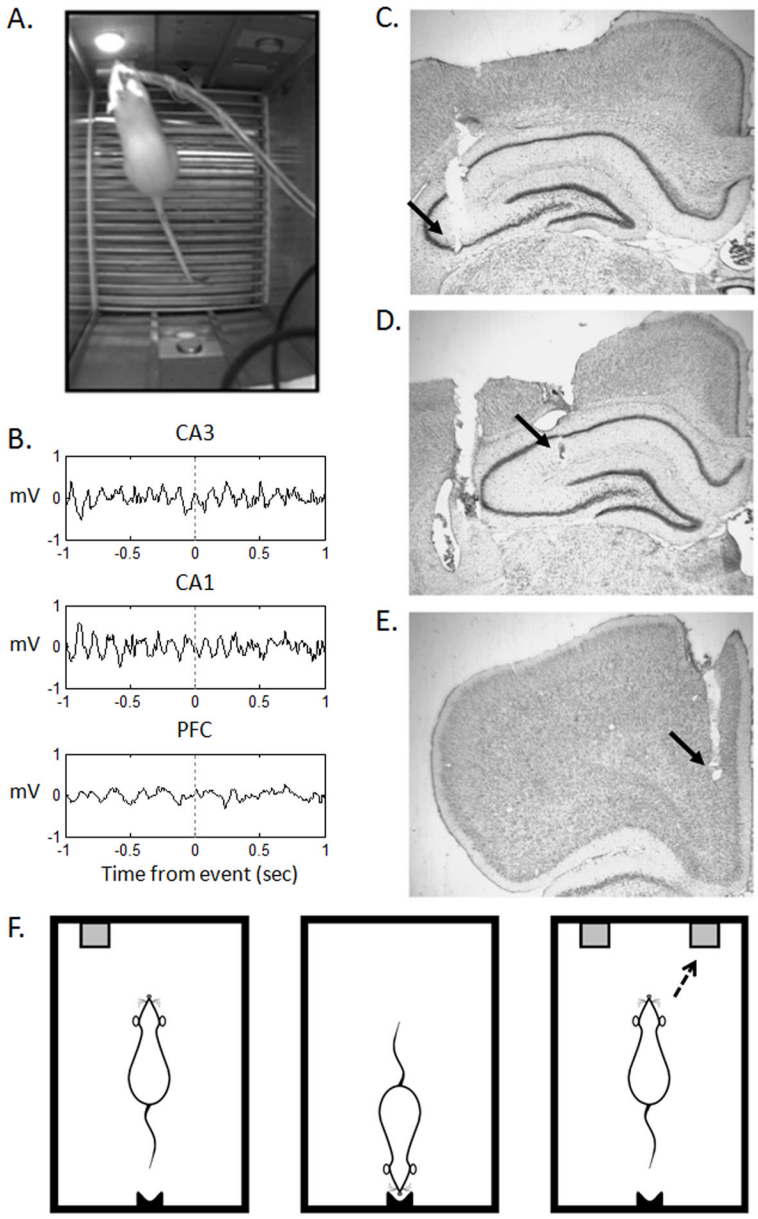

Figure 1.

Behavior and electrophysiological recording. A. Rat engaged in a DNMS trial, during the sample lever press. Depth EEG was recorded via a cable visible in the picture. B. Example EEG traces from each of the recorded areas in a control rat are shown around the moment of a sample lever press (dotted line). C–E. Representative thionin-stained coronal sections illustrating electrode placements in the CA3 (C), CA1 (D), and PFC (E). Arrows indicate the locations of the deepest electrode. F. Outline of the DNMS task. The rat was required to press a sample lever ("sample"; left lever in this case), followed by an imposed delay period during which the rat had to break an infrared beam on the opposite wall. After the imposed delay the rat was required the press the opposite lever ("nonmatch"; right lever in this case indicated by a dashed arrow) to gain a food reward.

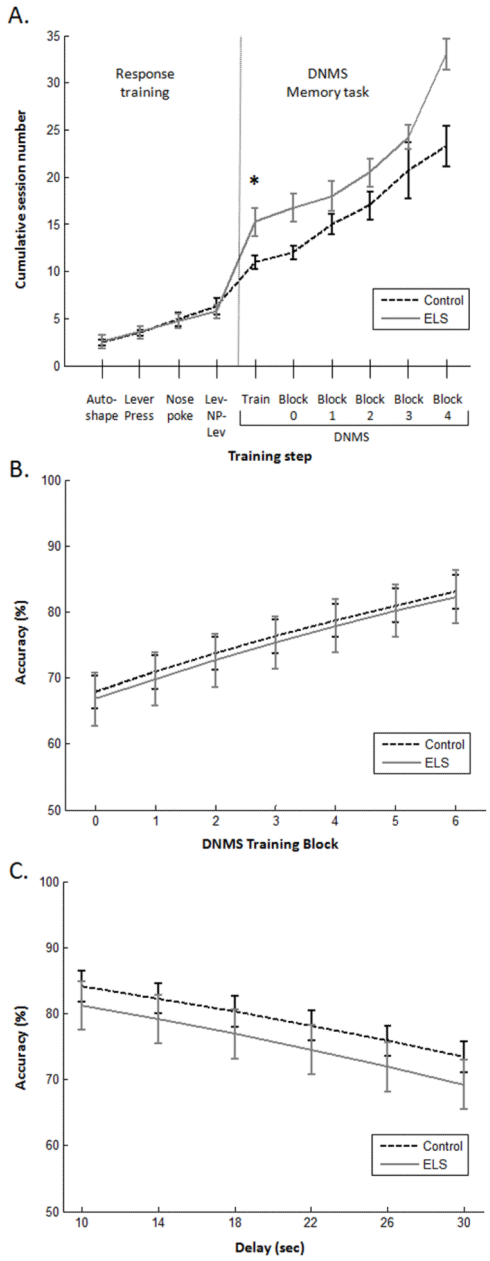

Figure 2.

Behavioral performance. A. Learning progression during training, shown as the average cumulative session number (± SEM) to reach criteria and advance to the next training step. Consecutive session types are listed on the x-axis. Because some rats did not complete criterion for all steps, Blocks 5 and 6 are not shown. Response training steps involved learning to press a lever for food reward ("autoshape", "lever press") and break an infrared beam (nosepoke) for food reward. The Lev-NP-Lev step involved an action sequence of pressing a randomly presented lever followed by nosepoke on the opposite wall, after which only the opposite lever from before was presented and had to be pressed. This prepared rats for the upcoming DNMS sequence in which both levers were presented after nosepoking to apply a memory component, as described in Figure 1*F* and in the Methods section. ELS rats

initially took longer to learn this task during the DNMS Train step (*p<0.01). B. Accuracy as a function of training block (± SEM), modeled using logistic regression. Despite adding longer delays to each consecutive block, accuracy increased over the course of training with no significant difference between the groups. C. Accuracy as a function of delay (± SEM; all blocks included), modeled using logistic regression. Accuracy decreased as delay increased.

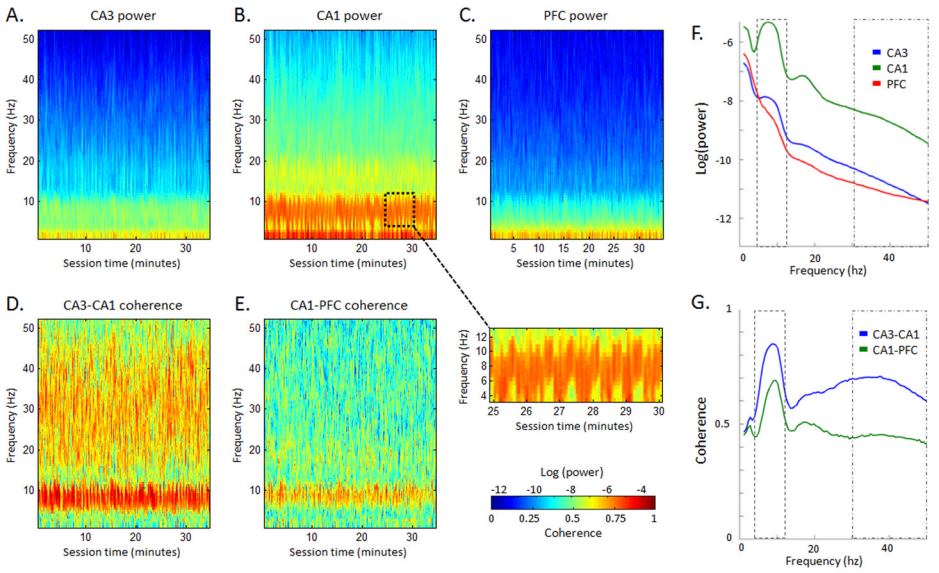

Figure 3.

Examples of power and coherence spectra. Power (A, B, C) and coherence (D, E) spectrograms from a single DNMS session are depicted, using a 1 sec non-overlapping window. The slightly striated appearance reflects the performance of repeated DNMS trials over the entire session. The zoomed inset panel arising from the dotted window in B shows this more clearly over the course of a five minute period, with a cyclic theta pattern corresponding to consecutive trials. Note the prominent theta (4–12 Hz) and gamma (30–50 Hz) activity particularly in the CA1 and CA3-CA1 panels (B, D). Theta and gamma band peaks are better reflected in the median power (F) and coherence (G) spectra examples, calculated from the spectrograms in A–E. Note the peaks in theta power, highest in CA1. Theta coherence is prominent between all structures, and notable gamma coherence band is evident between CA3-CA1 compared to CA1-PFC.

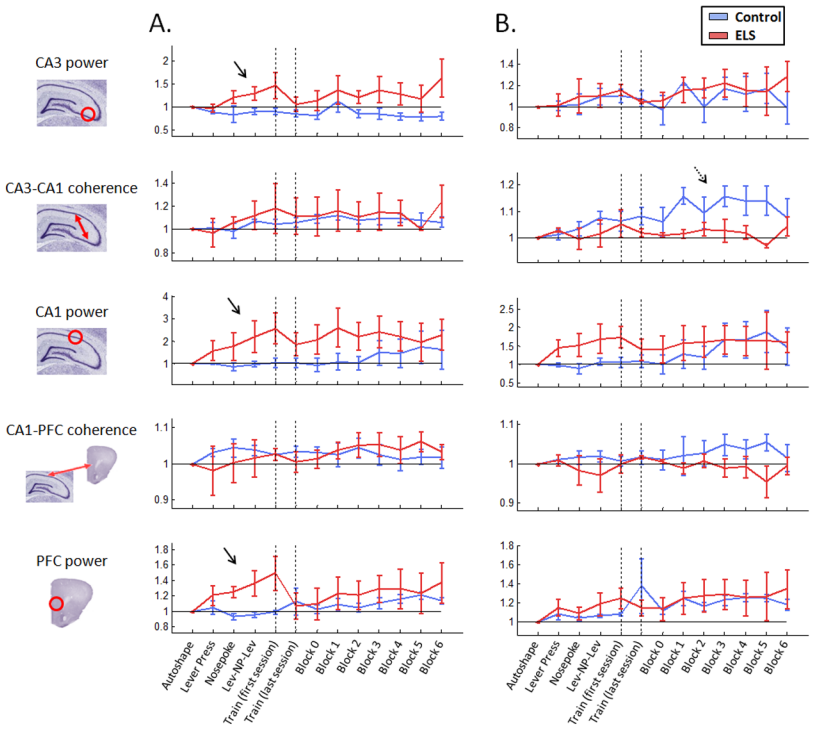

Figure 4.

Evolution of whole-session power and coherence during training. A. The progression of median theta power and coherence values across the progressive session training steps, averaged across rats in each group. ELS animals showed enhanced theta power in all structures during response training (solid arrows). B. Progression of median gamma power and coherence values across the session training steps. Control but not ELS animals showed an increase in CA3-CA1 coherence over the DNMS steps (dashed arrow).

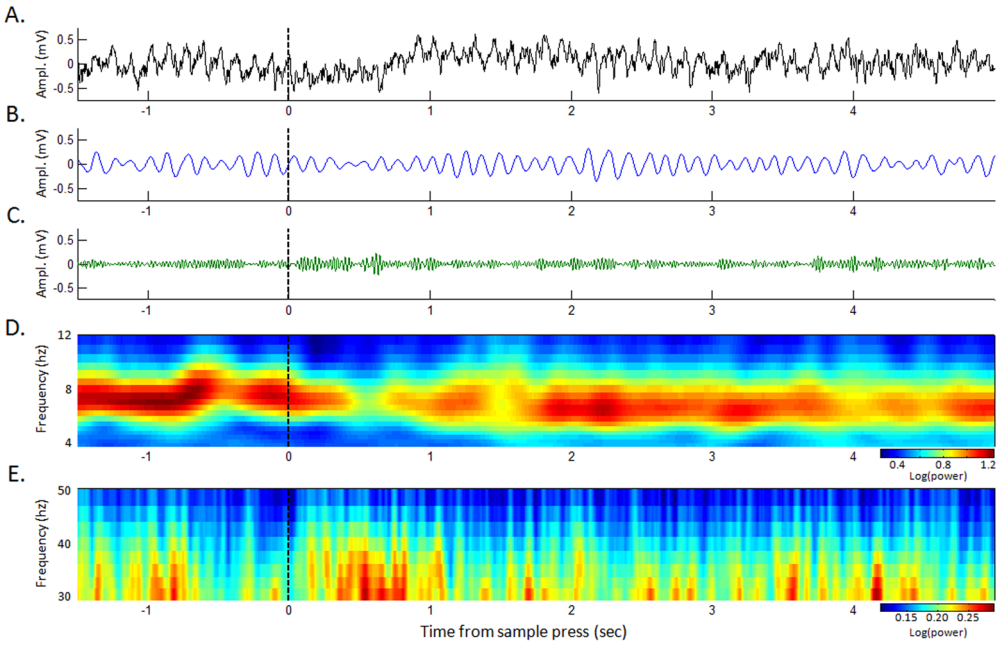

Figure 5.

Dynamic oscillations during real-time performance. A. Example of CA1 EEG recorded during the beginning of a DNMS trial (dashed line indicates the moment of the sample lever press). The same data is shown filtered in the 4–12 Hz theta band (B) and in the 30–50 Hz gamma band (C). Averaged power spectrogram over all completed trials (N=45) in a session by one rat (including the trial in A) are also shown for frequencies in the theta band (D) and gamma band (E). Spectrograms were averaged within frequency bands in each trial to produce dynamic traces for the analyses in Figures 6–8.

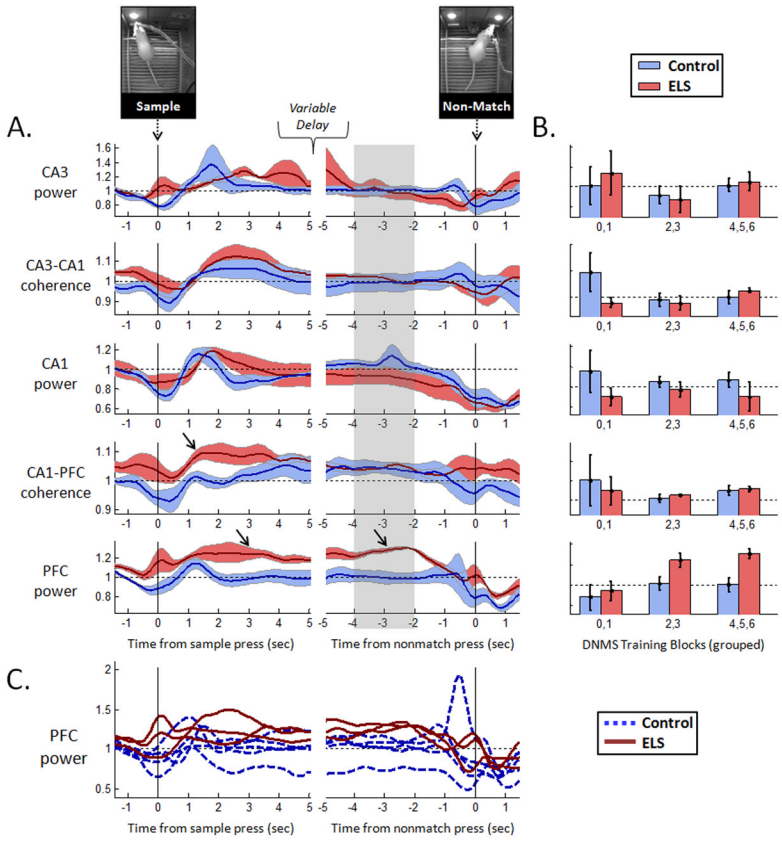

Figure 6.

Dynamic theta power and coherence during real-time performance of DNMS trials. A. Power and coherence were calculated within-subject, and are illustrated as colored envelopes bounded by the standard errors around the means (solid lines). Data on left is time-locked to the sample press, and data on the right to the match press (with variable delays between the two), revealing functional differences between control (blue) and ELS (red) rats when the envelopes diverge. ELS rats showed elevated PFC theta power from the beginning to the end of the trial (sample to match press), and increased CA1-PFC coherence following the sample press (solid arrows). B. Evolution of theta in the retrieval period (gray box in A) over the course of DNMS training, with training blocks grouped into three consecutive levels. C. PFC power data from individual rats used to produce the averaged data in A (last panel). Notice that all ELS rats showed consistently higher PFC power than controls in general, particularly before the match lever press.

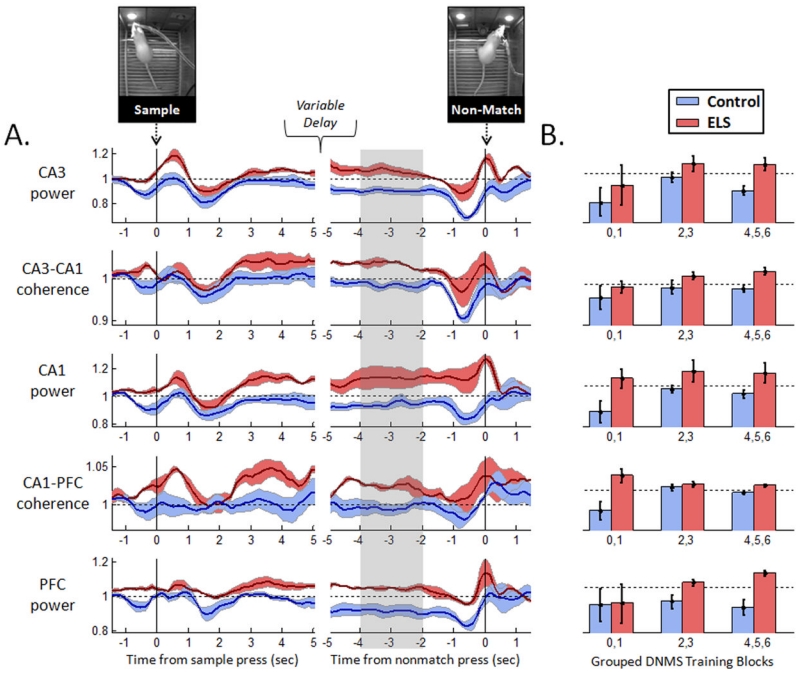

Figure 7.

Dynamic gamma power and coherence during real-time performance of DNMS trials. A. Powers and coherences were calculated similar to theta in Fig 6A. ELS rats showed elevated gamma power and coherence among practically all structures during the trials, which returned to control levels afterward. Most notably, ELS rats showed robustly increased CA3-CA1 gamma coherence and PFC gamma power shortly before the match press (memory retrieval phase). B. Evolution of gamma in the retrieval period (gray box in A) over the course of DNMS training, with blocks grouped into three consecutive levels.

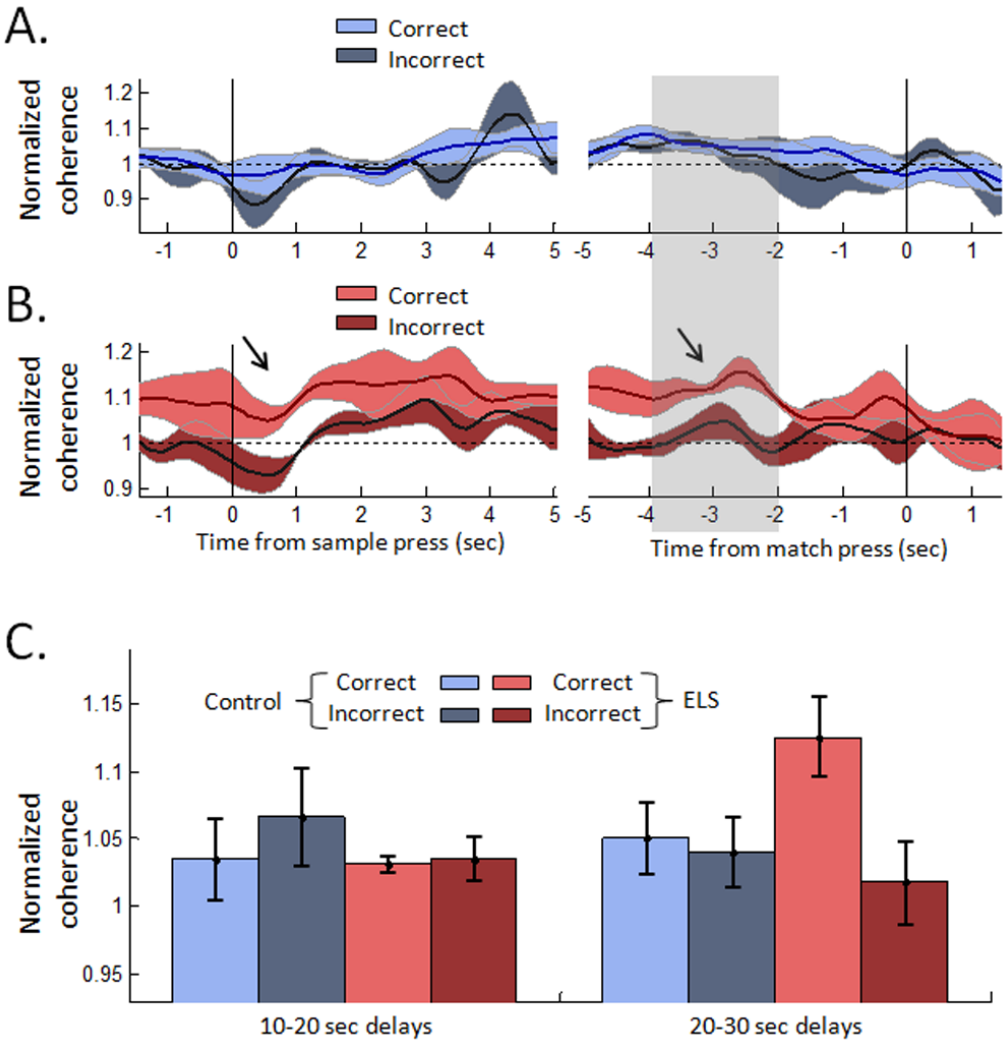

Figure 8.

Dynamic CA1-PFC theta coherence in correct and incorrect trials. A. In trials with 20–30 second delays, control rats did not show performance-related differences in CA1-PFC coherence between correct (light blue) and incorrect (dark blue). B. In trials with 20–30 second delays, ELS rats showed increased CA1-PFC coherence in correct trials (light red) relative to incorrect trials (dark red) particularly around the time of the sample press and prior to the match press (arrows). C. CA1-PFC theta coherence during retrieval (grey box in A, B) as a function of delay (all blocks included). The data is grouped into two delay levels and separated into correct and incorrect trials. Confirming A and B, CA1-PFC coherence is increased in correct trials compared to incorrect trials in trials with longer delays among ELS animals but not controls, suggesting that hippocampal-prefrontal interplay is particularly useful for this group when memory demand is high.